J Periodontal Implant Sci. 2022 Apr;52(2):141-154
https://doi.org/10.5051/jpis.2104360218
pISSN 2093-2278·eISSN 2093-2286

JPIS
Journal of Periodontal & Implant Science

Research Article
Periodontal Science

Check for updates

A murine periodontitis model using coaggregation between human pathogens and a predominant mouse oral commensal bacterium

Mengmeng Liu †, **Youngnim Choi** *

Department of Immunology and Molecular Microbiology, School of Dentistry and Dental Research Institute, Seoul National University, Seoul, Korea

OPEN ACCESS

Received: Aug 9, 2021
Revised: Oct 2, 2021
Accepted: Oct 25, 2021
ublished online: Dec 2, 2021

***Correspondence:**
Youngnim Choi
Department of Immunology and Molecular Microbiology, School of Dentistry and Dental Research Institute, Seoul National University, 101 Daehak-ro, Jongno-gu, Seoul 03080, Korea.
Email: youngnim@snu.ac.kr
Tel: +82-2-740-8643
Fax: +82-2-743-0311

†Current address: Shandong Provincial Key Laboratory of Oral Tissue Regeneration & Shandong Engineering Laboratory for Dental Materials and Oral Tissue Regeneration, School of Stomatology, Shandong University, Jinan, Shandong 250012, China

ORCID iDs
Mengmeng Liu
https://orcid.org/0000-0003-4580-8735
Youngnim Choi
https://orcid.org/0000-0002-6496-5560

Funding
This research was supported by grants (2017M3A9B6062986, 2018R1A5A2024418, and 2020R1A2C2007038) from the National Research Foundation (NRF) funded by the Ministry of Science and ICT, Korea.

ABSTRACT

Purpose: C57BL/6 mice, which are among the most common backgrounds for genetically engineered mice, are resistant to the induction of periodontitis by oral infection with periodontal pathogens. This study aimed to develop a periodontitis model in C57BL/6 mice using coaggregation between human pathogens and the mouse oral commensal *Streptococcus danieliae* (Sd).
Methods: The abilities of *Porphyromonas gingivalis* ATCC 33277 (Pg33277), *P. gingivalis* ATCC 49417 (Pg49417), *P. gingivalis* KUMC-P4 (PgP4), *Fusobacterium nucleatum* subsp. *nucleatum* ATCC 25586 (Fnn), and *F. nucleatum* subsp. *animalis* KCOM 1280 (Fna) to coaggregate with Sd were tested by a sedimentation assay. The Sd-noncoaggregating Pg33277 and 2 Sd-coaggregating strains, PgP4 and Fna, were chosen for animal experiments. Eighty C57BL/6 mice received oral gavage with Sd once and subsequently received vehicle alone (sham), Fna, Pg33277, PgP4, or Fna+PgP4 6 times at 2-day intervals. Mice were evaluated at 5 or 8 weeks after the first gavage of human strains.
Results: Fnn, Fna, and PgP4 efficiently coaggregated with Sd, but Pg33277 and Pg49417 did not. Alveolar bone loss was significantly higher in the PgP4 group at both time points (weeks 5 and 8) and in all experimental groups at week 8 compared with the sham group. The PgP4 group presented greater alveolar bone loss than the other experimental groups at both time points. A higher degree of alveolar bone loss accompanied higher bacterial loads in the oral cavity, the invasion of not only PgP4 but also Sd and Fna, and the serum antibody responses to these bacteria.
Conclusions: Periodontitis was successfully induced in C57BL/6 mice by oral infection with a *P. gingivalis* strain that persists in the oral cavity through coaggregation with a mouse oral commensal bacterium. This new model will be useful for studying the role of human oral bacteria-host interactions in periodontitis using genetically engineered mice.

Keywords: Animal models; Mice; Periodontitis; *Porphyromonas gingivalis*; *Streptococcus danieliae*

INTRODUCTION

A number of animal models are available for periodontitis. Animal models provide unique opportunities to test diverse hypotheses regarding the pathogenesis, prevention, and

JPIS Journal of Periodontal & Implant Science

Author Contributions
Conceptualization: Youngnim Choi; Data curation: Mengmeng Liu; Formal analysis: Mengmeng Liu, Youngnim Choi; Methodology: Mengmeng Liu; Project administration: Youngnim Choi; Supervision: Youngnim Choi; Writing - original draft: Mengmeng Liu; Writing - review & editing: Youngnim Choi.

Conflict of Interest
No potential conflict of interest relevant to this article was reported.

treatment of periodontitis, but no model is adequate to investigate all phases of periodontitis: (1) colonization; (2) invasion of gingival tissue; (3) the inflammatory response; (4) connective tissue breakdown and bone resorption; and (5) tissue repair [1]. Murine models are widely used due to their low cost, the ease of genetic engineering, and the availability of detailed knowledge on their genetics and immune systems [2]. Two methods commonly used to induce periodontitis in mice are oral gavage of periodontal pathogens and the placement of a ligature between 2 maxillary molars.

The ligature model rapidly induces gingival inflammation and alveolar bone loss at a known time (days 3–9 after ligature placement) in mice of any genetic background; thus, it is useful to study molecular mechanisms of periodontal inflammation and bone biology in periodontitis using diverse genetically engineered mice [3]. However, this model necessitates the use of germ-free mice to study human oral bacteria-host interactions. Furthermore, unlike human chronic periodontitis, most bone destruction occurs before the infiltration of helper T cells [3].

In an oral gavage model, an oral infection with periodontal pathogens, such as *Porphyromonas gingivalis*, induces increased inflammatory cytokine expression, the infiltration of leukocytes in gingival tissues, alveolar bone loss, and the serum immunoglobulin G (IgG) response against pathogens [1]. However, several strains, including C57BL/6, are resistant to periodontitis induction [4], although C57BL/6 is one of the most common backgrounds for genetically engineered mice. In addition, *P. gingivalis* is not a member of the indigenous oral microbiota in mice and is believed to reside only transiently in the oral cavity of mice [5]. Therefore, the oral gavage model is useful for studying the role of human oral bacteria-host interactions in periodontitis and systemic diseases, but has limited applicability to genetically engineered mice or studies of the colonization process of periodontal pathogens.

We previously reported the predominance of simple oral microbiota in C57BL/6 mice by a phylotype designated *Streptococcus* EU453973_s, which accounted for up to 94% of the total bacteria [6]. This phylotype is identical to *Streptococcus danieliae* (Sd), which was later isolated in the mouse gut [7], and this species has also been found to predominate the oral microbiota of mice of the 129/Ola × C57BL/6 background [8]. We hypothesized that human periodontal pathogens coaggregating with the murine oral commensal Sd could colonize the mouse oral cavity and might cause persistent infection of gingival tissues. The aim of this study was to develop a chronic periodontitis model in mice using the ability of *P. gingivalis* to coaggregate with Sd.

MATERIALS AND METHODS

Bacterial culture

Sd (DSM 26621; German Collection of Microorganisms and Cell Cultures, Braunschweig, Germany) was cultured in brain heart infusion broth microaerobically (2%–10% O_2) at 37°C. *Fusobacterium nucleatum* subsp. *nucleatum* ATCC 25586 (Fnn; American Type Culture Collection [ATCC], Manassas, VA, USA), *F. nucleatum* subsp. *animalis* KCOM 1280 (Fna; Korean Collection for Oral Microorganisms, Gwangju, Korea), *P. gingivalis* ATCC 33277 (Pg33277; ATCC), *P. gingivalis* ATCC 49417 (Pg49417; ATCC), and *P. gingivalis* KUMC-P4 (PgP4) were anaerobically cultured in the appropriate media as previously described [9,10].

https://doi.org/10.5051/jpis.2104360218

Bacterial aggregation assay

Bacterial aggregation was determined by a sedimentation assay. The bacteria were suspended in coaggregation buffer (1 mM Tris [hydroxymethyl] aminomethane, 0.1 mM $CaCl_2$, 0.1 mM $MgCl_2$, 3.1 mM NaN_3, and 0.15 M NaCl adjusted to pH 8.0), and the optical density (OD) at 660 nm was adjusted to 0.25. Equal volumes (0.5 mL) of each bacterial suspension were mixed, and the initial OD of the mixtures was measured ($OD660_{T0}$). After 90 minutes of incubation at room temperature, the OD660 was measured again ($OD660_{T90}$). The percentage of autoaggregation or coaggregation was calculated as [$100\times(OD660_{T0}-OD660_{T90})/OD660_{T0}$].

Confocal microscopy of coaggregated bacteria

Two bacterial species were labeled with different fluorescent dyes: carboxyfluorescein diacetate succinimidyl ester (CFSE; Molecular Probes, Carlsbad, CA, USA) and pHrodo™ Red succinimidyl ester (pHrodoRed; Thermo Fisher Scientific, Waltham, MA, USA). The labeled bacteria were resuspended in a coaggregation buffer, and the OD660 was adjusted to 0.25. Equal volumes (0.5 mL) of each bacterial suspension were seeded onto 12-mm cover slides in 24-well plates, and incubated at room temperature for 2 hours. The cover slides were washed with phosphate-buffered saline (PBS), mounted in mounting medium (pH 4.5; Biomeda, Foster City, CA, USA), and examined using a confocal microscope (Carl Zeiss, Jena, Germany).

Analysis of bacterial invasion of immortalized murine oral keratinocyte (IMOK) cells

An IMOK cell line [11], a kind gift from Professor Garrett-Sinha at the State University of New York at Buffalo, was maintained in CnT-Prime epithelial cell culture medium (Carl Zeiss).

IMOK cells (5×10^4 cells) were cultured in glass-bottomed dishes (WPI, Sarasota, FL, USA) for 24 hours. IMOK cells were infected with CFSE/pHrodoRed double-labeled Fna, Sd, Pg33277, or PgP4 at a multiplicity of infection of 1,000 for 4 hours. Time-lapse imaging was performed using a 3D Cell-Explorer fluorescence microscope (Nanolive SA, Tolochenaz, Switzerland).

Induction of periodontitis in mice

The mouse experiments were performed with approval from the Seoul National University Animal Care and Use Committee (No. SNU-190115-2-2) and conducted in accordance with the Laboratory Animals Act 9025 of the Republic of Korea. Six-week-old C57BL/6 mice (Orient, Seongnam, Korea), randomly divided into 5 groups, group-housed, and kept under specific pathogen-free conditions in the Laboratory Animal Facility at the School of Dentistry, Seoul National University. After a 7-day resting period, all mice received oral gavage of Sd (2×10^9 cells). Three days later, mice received oral gavage with 2×10^9 Fna, Pg33277, PgP4, or PgP4+Fna cells, or vehicle alone (sham) in 100 μL of PBS containing 2% carboxymethyl cellulose 6 times at 2-day intervals. Half of the mice were euthanized at 5 weeks, and the other half were euthanized at 8 weeks after the first oral gavage of human strains. Oral bacteria were collected using cotton swabs. Blood samples collected via cardiac puncture were subjected to centrifugation in BD Microtainer® tubes (BD Diagnostic Systems, Sparks, MD, USA) to obtain sera. Saliva was collected for 10 minutes after an intraperitoneal injection of pilocarpine (5 mg/kg of body weight). The maxillae and mandibles were also collected. Experiments were performed in 2 independent sets (n=5/group/time point for the first set and n=3/group/time point for the second set), and the data were combined. The mandibles for histology and the baseline samples of oral bacteria, saliva, and sera were obtained only from the second set of experiments.

https://doi.org/10.5051/jpis.2104360218

Measurement of alveolar bone loss

One hemimaxilla per mouse was scanned with micro-computed tomography (Bruker, Billerica, MA, USA). The acceleration potential of the X-ray generator was set at 80 kV with the beam current at 80 μA. The X-ray source was combined with a 2-dimensional detector running at a shutter speed of 1,100 ms to produce an image with a voxel size of 18×18×18 μm. A sagittal image depicting all cups of 3 molars was obtained, and the distances between the cementoenamel junction and alveolar bone crest at 6 sites (the mesial and distal aspects of the first, second and third molars) per mouse were measured in a blinded fashion with DataViewer software (Bruker).

Quantitative polymerase chain reaction (qPCR) of oral bacteria

Under general anesthesia with Zoletil (15 mg/kg, Virbac Korea, Seoul, Korea), the oral cavity was swabbed using a sterile cotton swab for 30 seconds. Genomic DNA was extracted using a PowerSoil® DNA Isolation Kit (Mo BIO Laboratories, Carlsbad, CA, USA). Real-time qPCR was performed in a total volume of 20 μL, including 2 μL of template DNA and species-specific primers, using the following cycling conditions: 4-minute incubation at 95°C followed by 40 cycles of denaturation at 95°C for 15 seconds, annealing at 60°C for 15 seconds, and extension at 70°C for 33 seconds. The primer sequences are listed in **Table 1**. The number of bacteria in each sample was calculated with a standard curve generated using 10-fold serial dilutions of genomic DNA (10^7 to 1 cells) of each species. PCR was performed in triplicate for each sample.

Histological evaluation

The left and right mandibles were fixed in a zinc-based fixative, decalcified, and then embedded in paraffin. A series of coronal (buccolingual) sections of the molars was made at 4 μm and subjected to staining with hematoxylin and eosin and *in situ* hybridization using Sd-, Fna-, and *P. gingivalis*-specific probes.

For *in situ* hybridization, species-specific probes were prepared by PCR amplification using the gDNA of each species and specific primers (**Table 1**) followed by labeling with digoxigenin-dUTP using a commercial kit (Roche Applied Science, Penzberg, Germany). After the specificity and sensitivity of each labeled probe were tested (**Supplementary Figure 1**), *in situ* hybridization was performed as previously described [12].

Table 1. Primer sequences used for polymerase chain reaction in the present study

Target	Orientation	Sequence (5′-3′)	Application
S. danieliae 16S rRNA	Forward	CGTAGGTCCCGAGCGTTATC	Quantitative polymerase chain reaction
	Reverse	TCTACGCATTCCACCGCTAC	
F. nucleatum 16S rRNA	Forward	TGTAGTTCCGCTTACCTCTTCAG	
	Reverse	AAGCGCGTCTAGGTGGTTATGT	
P. gingivalis 16S rRNA	Forward	AGGCAGCTTGCCATACTGCG	
	Reverse	ACTGTTAGCAACTACCGATGT	
P. gingivalis ATCC 33277 FimA	Forward	CGCATGGCTTTCACCGAAAT	
	Reverse	GCATTTACGAGTGTTGCCCC	
P. gingivalis KUMC-P4 FimA	Forward	TTC AGC GGT GCT TAT ACC CC	
	Reverse	CTG AGC GTA TGT GCT CTC CA	
S. danieliae 16S rRNA	Forward	CGTAGGTCCCGAGCGTTATC	Probe for *in situ* hybridization
	Reverse	TCTACGCATTCCACCGCTAC	
F. nucleatum 16S rRNA	Forward	AACTTAGGTTTGGGTGGCGG	
	Reverse	TGCTGGATCAGACTCTTGGT	
P. gingivalis 16S rRNA	Forward	TGCAACTTGCCTTACAGAGG	
	Reverse	ACTCGTATCGCCCGTTATTC	

https://doi.org/10.5051/jpis.2104360218

To evaluate bacterial invasion of gingival tissue, 8–11 sites per group were photographed and given a score of 0–6 by assigning 3 points each to the epithelium and lamina propria as follows: 1, signals visible only at high magnification; 2, signals visible at low magnification; and 3, strong signals at low magnification. The scoring was performed by 2 investigators and averaged.

Enzyme-linked immunosorbent assay

To determine the levels of antibodies against the bacteria in the saliva and sera, high-binding 96-well plates were coated with 0.1 μg/well bacterial lysate of each species in PBS overnight at 4°C. The lysate of *P. gingivalis* was prepared by mixing equal amounts of Pg33277 and PgP4 strains. After blocking with 1% bovine serum albumin in PBS, the plates were incubated with saliva (1:20 dilution) or sera (1:100 dilution for immunoglobulin A [IgA] and 1:500 dilution for IgG). The remaining procedures were performed as previously described [13]. For the standard, 2 columns in each plate were coated with serially diluted (50 ng/mL to 1.56 ng/mL) mouse IgG1 (BD Diagnostic Systems) or IgA (BD Diagnostic Systems) instead of the antigen. The levels of specific antibodies were calculated using an equation generated from the standard curve.

Statistical analysis

The results of the coaggregation assay were analyzed with the Student *t*-test. Differences between the sham and experimental groups or between weeks 5 and 8 in animal experiments were determined using the Mann–Whitney *U* test, except for alveolar bone loss. The alveolar bone loss data were normally distributed and were analyzed using the Student *t*-test. All analyses were 2-tailed and were performed with SPSS version 25 (IBM, Armonk, NY, USA). The threshold of statistical significance was set at $P<0.05$.

RESULTS

Efficient coaggregation of Sd with Fna and PgP4

To identify periodontopathic strains of human origin that can coaggregate with murine oral commensal Sd, 3 *P. gingivalis* and 2 *F. nucleatum* strains were tested. The autoaggregation ability of each strain was not significantly different from that of Sd. When the coaggregation of Sd with each periodontopathic strain was examined, Fnn, Fna, and PgP4 showed significantly higher levels of aggregation than that of Sd alone. However, Pg33277 and Pg49417 did not. The mixture of Sd, PgP4, and Fna did not increase coaggregation compared with the 2-strain mixtures (**Figure 1A**).

The coaggregation of Sd with human strains was further examined by confocal microscopy after staining with different fluorescent dyes. The coaggregation of Sd with *F. nucleatum* resulted in huge aggregates, which were more evident with Fna. Among the tested *P. gingivalis* strains, PgP4 obviously presented the greatest coaggregation with Sd. The coaggregation of Fna with PgP4 resulted in smaller aggregates than those of Fna with Sd (**Figure 1B**).

Bacterial invasion of IMOK cells

Bacterial invasion of keratinocytes is one of the important mechanisms in gingival tissue infection [14]. Based on the results of the coaggregation tests, Sd, Fna, Pg33277, and PgP4 were assayed to investigate whether these strains could invade IMOK cells using CFSE/pHrodoRed double-stained bacteria. The pHrodoRed dye becomes fluorescent in acidic pH

https://doi.org/10.5051/jpis.2104360218

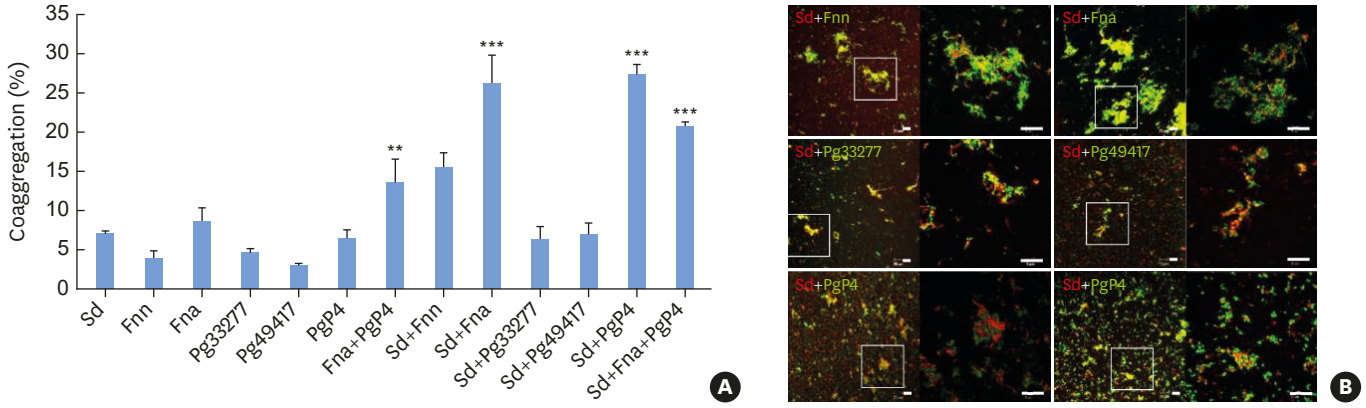

Figure 1. Autoaggregation and coaggregation of human and mouse oral bacteria. (A) The autoaggregation and coaggregation of bacterial cells were evaluated by sedimentation assays. Each column represents the mean and standard error of the mean for 5 experiments performed in triplicate. (B) Coaggregation of 2 species stained with different fluorescent dyes was examined by confocal microscopy. pHrodoRed-stained Sd (red) was mixed with CFSE-stained Fnn, Fna, Pg33277, Pg49417, or PgP4 (green). pHrodoRed-stained Fna (red) was mixed with CFSE-stained PgP4 (green). Representative images from 3 independent experiments are shown. Scale bars: 20 μm.
Sd: *S. danieliae*, Fnn: *F. nucleatum*. subsp. *nucleatum* ATCC 25586, Fna: *F. nucleatum*. subsp. *animalis* KCOM 1280, Pg33277: *P. gingivalis* ATCC 33277, Pg49417: *P. gingivalis* ATCC 49417, PgP4: *P. gingivalis* KUMC-P4.
$^{**}P<0.005$; $^{***}P<0.0005$ compared with the autoaggregation of Sd alone by the *t*-test.

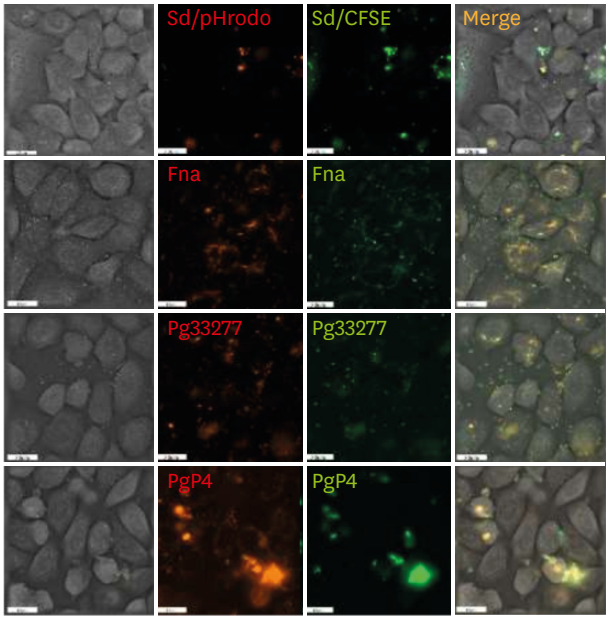

Figure 2. Bacterial invasion of IMOK cells. IMOK cells were infected with CFSE/pHrodoRed double-stained Sd, Fna, Pg33277, or PgP4 at a multiplicity of infection of 1,000 for 4 hours. The IMOK cells were then live imaged with time-lapse on a 3D Cell Explorer microscope (×600). Representative results of 2 independent experiments with similar results are shown. Each panel represents an appropriately selected section from serial stacks taken on the z-axis to visualize intracellular and extracellular bacteria. The bacteria in yellow represent intracellular bacteria. Scale bars: 20 μm.
IMOK: immortalized murine oral keratinocyte, Sd: *S. danieliae*, Fnn: *F. nucleatum*. subsp. *nucleatum* ATCC 25586, Fna: *F. nucleatum*. subsp. *animalis* KCOM 1280, Pg33277: *P. gingivalis* ATCC 33277, Pg49417: *P. gingivalis* ATCC 49417, PgP4: *P. gingivalis* KUMC-P4.

conditions, as in endosomes. Therefore, bacteria with pHrodoRed fluorescence indicate an intracellular location. The human strains presented clear differences in the frequency of pHrodoRed fluorescence from Sd (**Figure 2** and **Supplementary Video 1-4**).

https://doi.org/10.5051/jpis.2104360218

JPIS Journal of Periodontal & Implant Science

Increased alveolar bone loss by PgP4 along with increased oral bacteria in C57BL/6 mice

Although we previously reported the predominance of Sd in the oral microbiota of C57BL/6 mice, the oral microbiota of mice can differ depending on the source. To compare the ability of the Sd-coaggregating (Fna and PgP4) and Sd-noncoaggregating (Pg33277) strains to induce periodontitis in C57BL/6 mice, all mice received oral gavage of Sd once instead of antibiotic treatment. Subsequently, the mice received vehicle alone (sham), Fna, Pg33277, PgP4, or Fna+PgP4 6 times at 2-day intervals and were then evaluated 5 or 8 weeks after the first gavage (**Figure 3A**). Alveolar bone loss significantly increased at week 8 compared with week 5 in most groups, including the sham group. Compared with the sham group, the PgP4 group had higher alveolar bone loss at both time points, but other experimental groups presented increased alveolar bone loss only at week 8. In addition, the PgP4 group showed significantly greater alveolar bone loss than the other experimental groups at both time points (**Figure 3B and C**).

When the presence of human strains in the murine oral cavity was examined by qPCR, only hundreds of copies of Fna and none of *P. gingivalis* were detected at baseline, but both species significantly increased at week 8 in all groups, suggesting cross-cage contamination. At week 8, Fna significantly increased in all experimental groups, while *P. gingivalis* increased only in the *P. gingivalis*-inoculated groups compared with the sham group. Interestingly, Sd also increased in

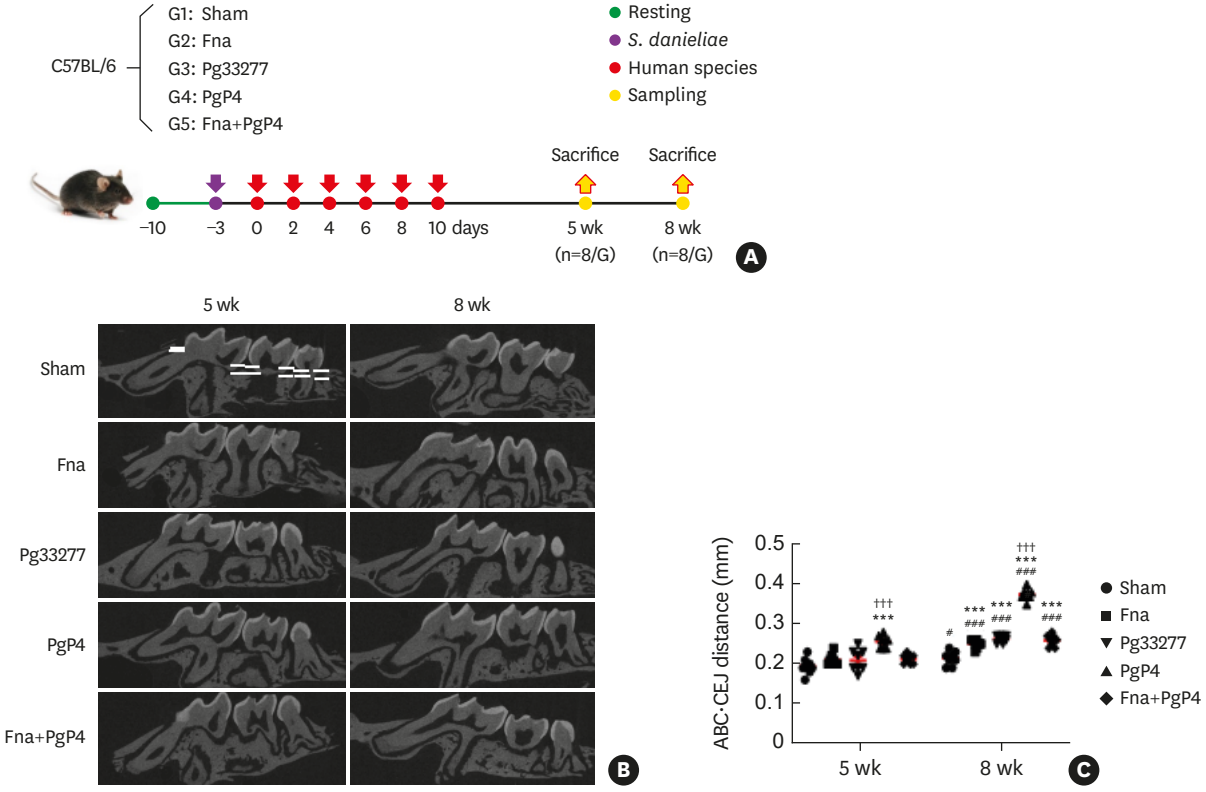

Figure 3. Increased alveolar bone loss by PgP4 in C57BL/6 mice. (A) The overall outline of the animal experiments. (B) Representative sagittal images of alveolar bones at the hemimaxilla scanned with microcomputed tomography. (C) Distances from the CEJ to the ABC at 6 sites marked with white lines in B were measured. Red lines indicate mean values.
Fna: *F. nucleatum*. subsp. *animalis* KCOM 1280, Pg33277: *P. gingivalis* ATCC 33277, PgP4: *P. gingivalis* KUMC-P4, CEJ: cementoenamel junction, ABC: alveolar bone crest.
$^{\#}P<0.05$, $^{\#\#\#}P<0.0005$ compared with week 5 by the *t*-test. $^{**}P<0.005$, $^{***}P<0.0005$ compared with the sham group by *t*-test. $^{\dagger\dagger\dagger}P<0.0005$ compared with other experimental groups by analysis of variance with Bonferroni-adjusted *post hoc* tests.

https://doi.org/10.5051/jpis.2104360218

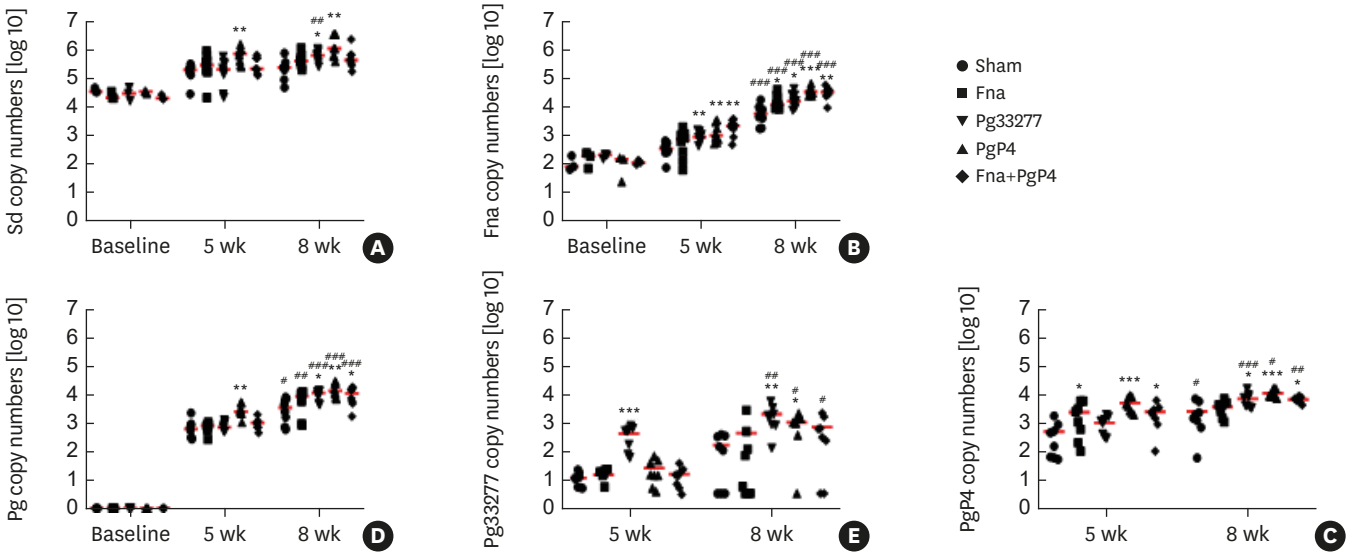

Figure 4. Successful colonization of human strains in C57BL/6 mice. The copy numbers of Sd, Fna, or Pg in the total DNA of oral swabs were determined by qPCR. (G, H). The copy numbers of Pg33277 and PgP4 in the total DNA of oral swabs were determined by qPCR. The horizontal lines indicate the median values.
Sd: *S. danieliae*, Fna: *F. nucleatum*. subsp. *animalis* KCOM 1280, Pg33277: *P. gingivalis* ATCC 33277, PgP4: *P. gingivalis* KUMC-P4, qPCR: quantitative polymerase chain reaction.
$^{\#}P<0.05$, $^{\#\#}P<0.005$, $^{\#\#\#}P<0.005$ compared with week 5 by the Mann-Whitney *U* test. $^{*}P<0.05$, $^{**}P<0.005$, $^{***}P<0.005$ compared with the sham group by the Mann-Whitney *U* test.

all groups at week 8 compared with the baseline, and the Pg33277 and PgP4 groups presented a greater increase than the sham group (**Figure 4A-C**). To clarify which strain of *P. gingivalis* was detected in the oral cavity, qPCR was performed using strain-specific primers targeting the FimA gene. The Pg33277 and PgP4 strains were detected at the highest level in the Pg33277 and PgP4 groups, respectively, at both time points. Only 4 to 81 copies of Pg33277 were detected at week 5 in the animals that did not receive Pg33277, but Pg33277 significantly increased in all *P. gingivalis*-inoculated groups at week 8 compared with week 5 (**Figure 4D**). In contrast, 61 to 6,440 copies of PgP4 were detected at week 5, even in the animals that did not receive PgP4 (**Figure 4E**).

Gingival inflammation and bacterial invasion of gingival tissues

Bacterial invasion of gingival tissues is an important step in the initiation of periodontitis. The presence of bacteria within the gingival tissue was examined by *in situ* hybridization using Sd-, Fna-, and *P. gingivalis*-specific probes and scored using arbitrary indexes (**Figure 5A** and **Supplementary Figure 2**). The invasion of Sd was detected at low levels in only a few sites at week 5, but Sd was more commonly detected at week 8. Strong Fna signals (≥4) were detected in a few sites at week 5 but were commonly detected in all groups regardless of Fna administration at week 8. Similarly, strong signals of *P. gingivalis* were detected in several sites regardless of the group at week 8. Importantly, both Fna and *P. gingivalis* were detected in all sites of the PgP4 group (**Figure 5B-D**).

Antibody responses to commensal versus periodontopathic bacteria

To gain insights into the antibody responses to commensal versus periodontopathic bacteria, the concentrations of salivary IgA (sIgA), serum IgA, and serum IgG against the 3 species were determined by enzyme-linked immunosorbent assays. At baseline, all animals had anti-Sd sIgA, but the other antibodies were detected in a few or no animals. The antibodies against each bacterial species significantly increased in all groups at week 8 compared with the baseline. In general, Sd induced high sIgA but low serum IgG responses compared with other species,

https://doi.org/10.5051/jpis.2104360218

JPIS Journal of Periodontal & Implant Science

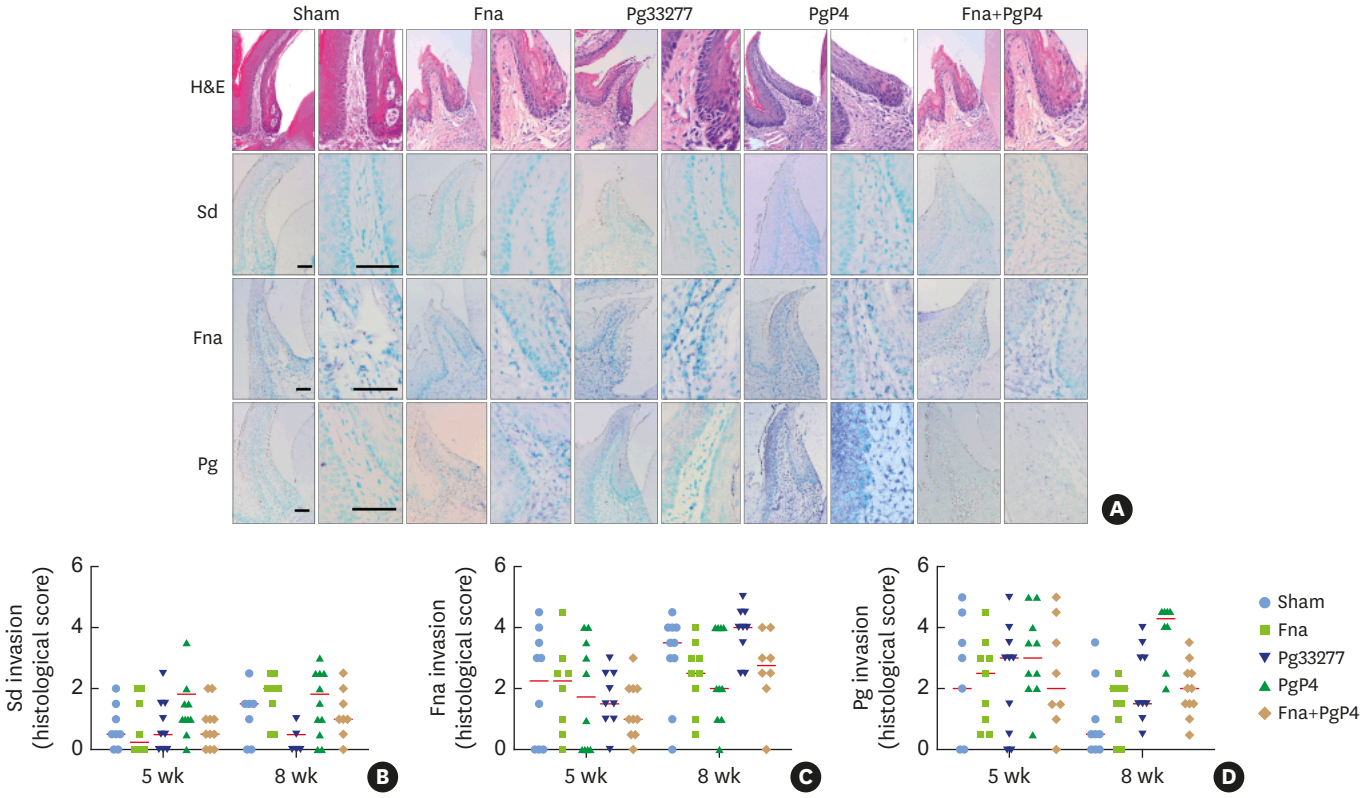

Figure 5. Gingival inflammation and bacterial invasion of gingival tissues. Sections of gingival tissues were subjected to hematoxylin and eosin staining and *in situ* hybridization using Sd-, Fna-, and *P. gingivalis*-specific probes. (A) Representative images of gingival tissues obtained at week 8 are shown. Scale bars: 50 μm. (B) The gingival inflammation index was scored by assigning 1 point each to inflammatory infiltration, vasodilation, and degradation of collagen fibers. (C-E) Bacterial signals in the epithelium and lamina propria were scored 0–3 (0, no signal; 1, signals visible only at high magnification; 2, signals visible at low magnification; 3, strong signals at low magnification) and presented as the sum. The horizontal lines indicate the median values.
H&E: hematoxylin and eosin, Fna: *F. nucleatum*. subsp. *animalis* KCOM 1280, Pg33277: *P. gingivalis* ATCC 33277, PgP4: *P. gingivalis* KUMC-P4, Sd: *S. danieliae*.

whereas Fna and *P. gingivalis* efficiently induced both sIgA and serum IgG responses. The serum IgA response well reflected the increased amount of each species in the oral cavity (**Figure 6**).

DISCUSSION

Here, we present a modified oral gavage model of periodontitis in which human periodontopathic strains coaggregating with mouse oral commensal Sd successfully induced alveolar bone loss in C57BL/6 mice. Importantly, this is a chronic model because periodontitis progressed over weeks (week 5 vs. week 8) along with increases in the bacterial load, bacterial invasion of gingival tissues, and serum antibody responses.

F. nucleatum is known to coaggregate with several oral streptococci, including *S. sanguinis*, *S. gordonii*, and *S. oralis* [15]. The partnership between *P. gingivalis* and *S. gordonii* is also well known [16]. Among the tested *F. nucleatum* and *P. gingivalis* strains, Fna and PgP4 presented substantial coaggregation with Sd, while Pg33277 and Pg49417 did not. Although the specific molecules involved in the coaggregation between PgP4 and Sd are not clear, *P. gingivalis* binds to *S. gordonii* through the major fimbrial protein FimA, and variation in the FimA sequences between Pg33277 and PgP4 has been documented [16,17]. *F. nucleatum* is known as a bridging colonizer that helps late-colonizing *P. gingivalis* adhere to early-colonizing streptococci.

https://doi.org/10.5051/jpis.2104360218

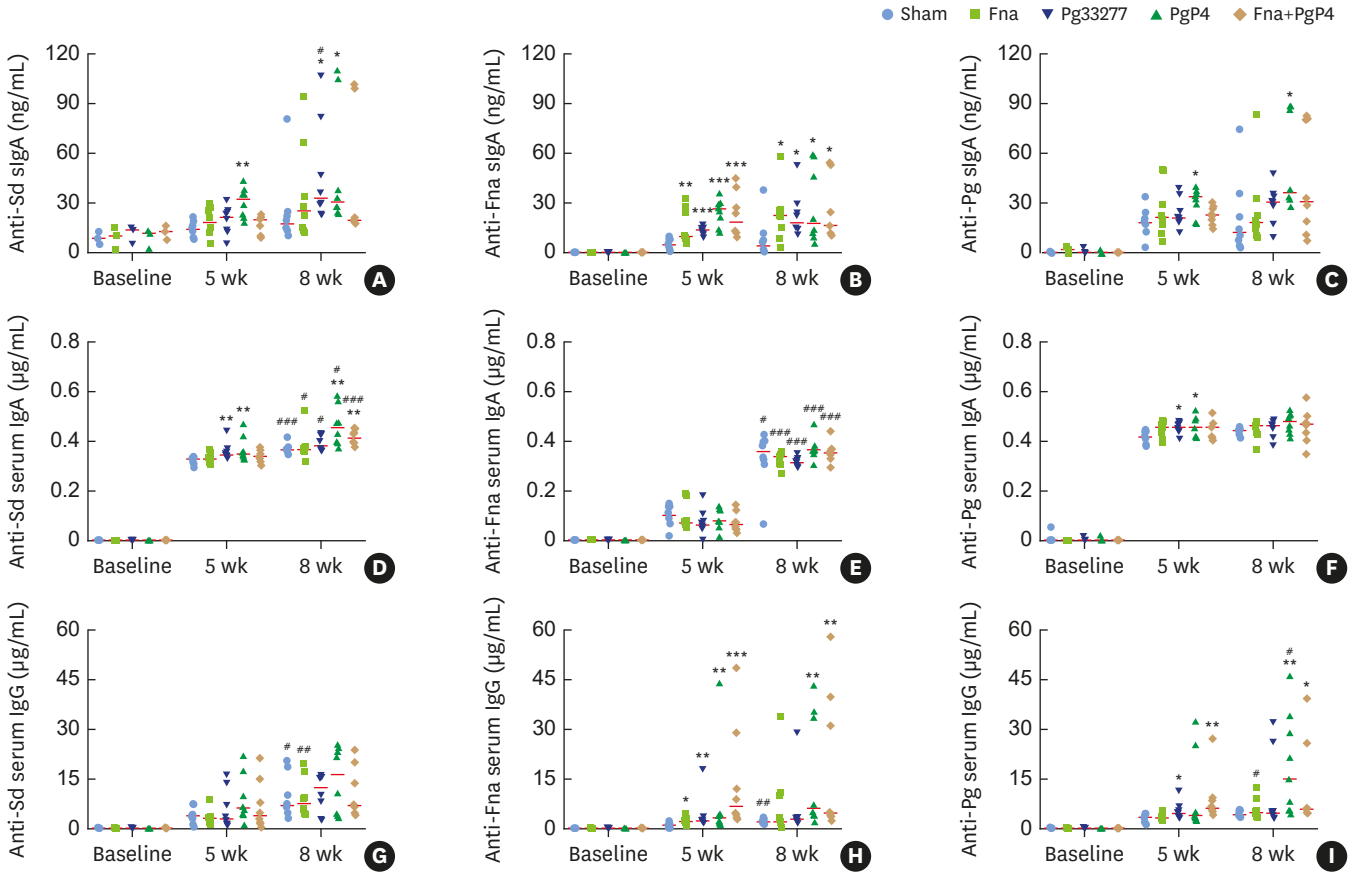

Figure 6. Antibody responses to commensal versus periodontopathic bacteria. The levels of sIgA, serum IgA, and serum IgG against Sd, Fna, and Pg were measured by enzyme-linked immunosorbent assays using the lysate of each species as antigens. The horizontal lines indicate the median values.
Sd: *S. danieliae*, sIgA: salivary immunoglobulin A, Fna: *F. nucleatum*. subsp. animalis KCOM 1280, Pg: *P. gingivalis*, Pg33277: *P. gingivalis* ATCC 33277, PgP4: *P. gingivalis* KUMC-P4, IgA: serum immunoglobulin A, IgG: immunoglobulin G.
$^{\#}P<0.05$, $^{\#\#}P<0.005$, $^{\#\#\#}P<0.005$ compared with week 5 by Mann-Whitney *U* test. $^{*}P<0.05$, $^{**}P<0.005$, $^{***}P<0.005$ compared with the sham group by the Mann-Whitney *U* test.

However, Fna did not enhance the coaggregation of PgP4 with Sd. Fna and PgP4 may compete for the same adhesin of Sd.

In the conventional oral gavage model, suppression of mouse oral commensal bacteria by antibiotic treatment is recommended to enhance the pathologic effect of human strains. In this modified model, however, mice received a mouse oral commensal Sd instead of antibiotic treatment. The quantitation results of each species and strain in the oral swabs indicated that not only the coaggregation ability with Sd, but also immune subversion activities, were important to gain a foothold in the oral cavity. The low levels of Fna detected at baseline must represent indigenous *F. nucleatum* in the mouse oral cavity [6]. The increased detection of Fna and *P. gingivalis* in the oral swabs at week 8 compared with baseline and week 5 indicates the stable colonization and growth of these species in the mouse oral cavity. The detection of *P. gingivalis* in the sham and Fna groups indicates cross-cage contamination that seems to have occurred during the change of cages. Although cross-cage contamination is a limitation of this study, it enabled some interesting observations. Contaminated Pg33277 was detected at low levels at week 5, while substantial amounts of contaminated PgP4 were detected at that time. This suggests the importance of the ability to coaggregate with Sd in gaining an initial foothold in the mouse oral cavity. The presence of PgP4 seemed to have

https://doi.org/10.5051/jpis.2104360218

helped Pg33277 expand its niche in the oral cavities of the PgP4 and Fna+PgP4 groups, where Pg33277 significantly increased at week 8 compared with week 5. The colonization of Fna also seemed to depend on *P. gingivalis* because the groups that received Pg33277 or PgP4, but not the Fna group, had higher amounts of Fna than the sham group at week 5. The ability of *P. gingivalis* to evade the host defense system tilts the balance between the host and the microbes, altering the numbers and composition of the entire bacterial community [5,10,18]. This is consistent with the increase in the amount of Sd in the Pg33277 and PgP4 groups, which had higher levels of *P. gingivalis* than the sham group. Notably, the numbers of *P. gingivalis* and Fna detected in the oral cavity of mice were 2–3 orders of magnitude lower than those of Sd (approximately 0.01%–10%), although 6 times more cells were administered. The proportions of *P. gingivalis* and Fna observed in mice coincide with findings in humans [19]. Unfortunately, isolation of human strains from the mouse oral cavity was not attempted in this study, which would be needed to confirm stable colonization of these strains.

Although all experimental groups presented increased alveolar bone loss compared with the sham group at week 8, only the PgP4 group showed increased alveolar bone loss at week 5; this group also had even greater bone loss than the other experimental groups at week 8. *P. gingivalis* cannot induce periodontitis in germ-free mice [18]. We speculate that not only *P. gingivalis,* but also Sd and Fna, played a role in our model. Both the bacterial load in the oral cavity and invasion of gingival tissues of these bacteria seem to be important in periodontitis induction. PgP4 is expected to invade tissue efficiently through both transcellular and paracellular routes, based on its strong abilities to invade IMOK cells and to degrade tight junctions [20]. The opening of the paracellular route by PgP4 should promote the invasion of Sd and Fna. PgP4 may also promote the invasion of Sd via coaggregation. *In situ* hybridization revealed a tendency toward increased bacterial invasion in the PgP4 group. Antibody responses supported the findings of more extensive invasion by Sd and Fna in the PgP4 and Fna+PgP4 groups than in the sham group, as discussed below.

How the adaptive immune system recognizes oral bacteria and induces antibody responses remains unclear. Interestingly, all mice had sIgA, but neither serum IgA nor serum IgG, against Sd at baseline, which reflects an efficient defense strategy against commensal bacteria that rarely invade tissue. M-cell-like cells have been identified in the epithelium of palatine tonsil crypts [21]. The luminal microbes taken up by these cells may induce only a mucosal immune response (i.e., sIgA) in the tonsils to control colonization and tissue invasion. In contrast, tissue-invading microbes that are captured by dendritic cells distributed in the oral mucosa and delivered to the draining lymph nodes may preferentially induce a systemic immune response (i.e., serum IgA and IgG). There is a possibility that ingested bacteria induced systemic antibody responses through the gut. It has been reported that ingestion of *P. gingivalis* exacerbates dextran sodium sulfate-induced colitis in mice [22]. However, no body weight loss was observed in our study (**Supplementary Figure 3**), suggesting that the ingested bacteria did not induce colitis in the absence of other triggering factors, such as dextran sodium sulfate. Therefore, it is unlikely that bacteria translocated through the gut. The serum IgA response closely reflected the increased amount of each species in the oral cavity.

In conclusion, we successfully induced chronic periodontitis in C57BL/6 mice by oral infection of the PgP4 strain that coaggregates with a dominant mouse oral commensal bacterium. This new model will allow us to study the role of human oral bacteria-host interactions in periodontitis using genetically engineered mice. Furthermore, this model will be useful for studying new therapeutics that target human oral bacteria-host interactions.

https://doi.org/10.5051/jpis.2104360218

ACKNOWLEDGEMENTS

We acknowledge Professor Hyun-Man Kim at the Department of Cell and Developmental Biology for providing histologic expertise on gingival inflammation.

SUPPLEMENTARY MATERIALS

Supplementary Figure 1
Specificity and sensitivity tests of DIG-labeled probes for in situ hybridization. (A) To confirm the specificity of probes, denatured genomic DNA (100 ng) from various bacterial species, including Sd, Fna, Pg33277, PgP4, Td, Tf, Vd, Sg, Aj, Sa, Ec, was hybridized with 1 ng/μl of DIG-labeled Sd-, Fna-, or Pg-specific probe. (B) Sensitivity test. Various concentrations of the DIG-labeled probes and control DNA provided in the kit were detected with anti-DIG antibodies. The concentration whose signal intensity was equivalent to that of 5 ng/μL control DNA was chosen and used for in situ hybridization.

Click here to view

Supplementary Figure 2
Gingival inflammation and bacterial invasion of gingival tissues at week 5. Sections of gingival tissues were subjected to H&E staining and in situ hybridization using Sd-, Fna-, and Pg-specific probes. Representative images are shown.

Click here to view

Supplementary Figure 3
Body weight change compared with the base line.

Click here to view

Supplementary Video 1
Sd invasion into IMOK

Click here to view

Supplementary Video 2
Fna invasion into IMOK

Click here to view

Supplementary Video 3
PgP4 invasion into IMOK

Click here to view

https://doi.org/10.5051/jpis.2104360218

Supplementary Video 4
Pg33277 invasion into IMOK

Click here to view

REFERENCES

1. Graves DT, Kang J, Andriankaja O, Wada K, Rossa C Jr. Animal models to study host-bacteria interactions involved in periodontitis. Front Oral Biol 2012;15:117-32.
PUBMED | CROSSREF
2. Gurumurthy CB, Lloyd KC. Generating mouse models for biomedical research: technological advances. Dis Model Mech 2019;12:dmm029462.
PUBMED | CROSSREF
3. Marchesan J, Girnary MS, Jing L, Miao MZ, Zhang S, Sun L, et al. An experimental murine model to study periodontitis. Nat Protoc 2018;13:2247-67.
PUBMED | CROSSREF
4. Baker PJ, Dixon M, Roopenian DC. Genetic control of susceptibility to Porphyromonas gingivalis-induced alveolar bone loss in mice. Infect Immun 2000;68:5864-8.
PUBMED | CROSSREF
5. Hajishengallis G, Diaz PI. *Porphyromonas gingivalis*: Immune subversion activities and role in periodontal dysbiosis. Curr Oral Health Rep 2020;7:12-21.
PUBMED | CROSSREF
6. Chun J, Kim KY, Lee JH, Choi Y. The analysis of oral microbial communities of wild-type and toll-like receptor 2-deficient mice using a 454 GS FLX Titanium pyrosequencer. BMC Microbiol 2010;10:101.
PUBMED | CROSSREF
7. Clavel T, Charrier C, Haller D. *Streptococcus danieliae* sp. nov., a novel bacterium isolated from the caecum of a mouse. Arch Microbiol 2013;195:43-9.
PUBMED | CROSSREF
8. Lee J, Alam J, Choi E, Ko YK, Lee A, Choi Y. Association of a dysbiotic oral microbiota with the development of focal lymphocytic sialadenitis in IκB-ζ-deficient mice. NPJ Biofilms Microbiomes 2020;6:49.
PUBMED | CROSSREF
9. Baek KJ, Ji S, Kim YC, Choi Y. Association of the invasion ability of *Porphyromonas gingivalis* with the severity of periodontitis. Virulence 2015;6:274-81.
PUBMED | CROSSREF
10. Ji S, Shin JE, Kim YC, Choi Y. Intracellular degradation of *Fusobacterium nucleatum* in human gingival epithelial cells. Mol Cells 2010;30:519-26.
PUBMED | CROSSREF
11. Parikh N, Nagarajan P, Sei-ichi M, Sinha S, Garrett-Sinha LA. Isolation and characterization of an immortalized oral keratinocyte cell line of mouse origin. Arch Oral Biol 2008;53:1091-100.
PUBMED | CROSSREF
12. Choi YS, Kim YC, Baek KJ, Choi Y. *In situ* detection of bacteria within paraffin-embedded tissues using a digoxin-labeled DNA probe targeting 16S rRNA. J Vis Exp 2015;99:e52836.
PUBMED | CROSSREF
13. Lee A, Kim YC, Baek K, Alam J, Choi YS, Rheu Y, et al. *Treponema dentícola* enolase contributes to the production of antibodies against ENO1 but not to the progression of periodontitis. Virulence 2018;9:1263-72.
PUBMED | CROSSREF
14. Tribble GD, Lamont RJ. Bacterial invasion of epithelial cells and spreading in periodontal tissue. Periodontol 2000 2010;52:68-83.
PUBMED | CROSSREF
15. Bradshaw DJ, Marsh PD, Watson GK, Allison C. Role of *Fusobacterium nucleatum* and coaggregation in anaerobe survival in planktonic and biofilm oral microbial communities during aeration. Infect Immun 1998;66:4729-32.
PUBMED | CROSSREF
16. Rickard AH, Gilbert P, High NJ, Kolenbrander PE, Handley PS. Bacterial coaggregation: an integral process in the development of multi-species biofilms. Trends Microbiol 2003;11:94-100.
PUBMED | CROSSREF

17. Lamont RJ, El-Sabaeny A, Park Y, Cook GS, Costerton JW, Demuth DR. Role of the *Streptococcus gordonii* SspB protein in the development of *Porphyromonas gingivalis* biofilms on streptococcal substrates. Microbiology (Reading) 2002;148:1627-36.
PUBMED | CROSSREF
18. Hajishengallis G, Liang S, Payne MA, Hashim A, Jotwani R, Eskan MA, et al. Low-abundance biofilm species orchestrates inflammatory periodontal disease through the commensal microbiota and complement. Cell Host Microbe 2011;10:497-506.
PUBMED | CROSSREF
19. Baek K, Ji S, Choi Y. Complex intratissue microbiota forms biofilms in periodontal lesions. J Dent Res 2018;97:192-200.
PUBMED | CROSSREF
20. Baek KJ, Choi YS, Kang CK, Choi Y. The proteolytic activity of *Porphyromonas gingivalis* is critical in a murine model of periodontitis. J Periodontol 2017;88:218-24.
PUBMED | CROSSREF
21. Wu RQ, Zhang DF, Tu E, Chen QM, Chen W. The mucosal immune system in the oral cavity-an orchestra of T cell diversity. Int J Oral Sci 2014;6:125-32.
PUBMED | CROSSREF
22. Tsuzuno T, Takahashi N, Yamada-Hara M, Yokoji-Takeuchi M, Sulijaya B, Aoki-Nonaka Y, et al. Ingestion of *Porphyromonas gingivalis* exacerbates colitis via intestinal epithelial barrier disruption in mice. J Periodontal Res 2021;56:275-88.
PUBMED | CROSSREF

https://doi.org/10.5051/jpis.2104360218